COULD CELL MEMBRANES PRODUCE ACOUSTIC STREAMING? MAKING THE CASE FOR SYNECHOCOCCUS SELF-PROPULSION

KURT M. EHLERS, JAIR KOILLER

Abstract. Sir James Lighthill proposed in 1992 that acoustic streaming occurs in the inner ear, as part of the cochlear amplifier mechanism. Here we hypothesize that some of the most ancient organisms use acoustic streaming not only for self-propulsion but also to enhance their nutrient uptake. We focus on a motile strain of Synechococcus, a cyanobacteria whose mechanism for self-propulsion is not known. Molecular motors could work like piezoelectric transducers acting on the crystalline structure surrounding the outer cell membrane. Our calculations show that a traveling surface acoustic wave (SAW) could account for the observed velocities. These SAW waves will also produce a non-negligible Stokes layer surrounding the cell: motion within this region being essentially chaotic. Therefore, an AS mechanism would be biologically advantageous, enhancing localized diffusion processes and consequently, chemical reactions. We believe that acoustic streaming, produced by nanometer scale membrane vibrations could be widespread in cell biology. Other possible instances are yeast cells and erythrocytes. Flows generated by acoustic streaming may also be produced by silica coated diatoms along their raphe. We note that microelectromechanical (MEMS) acoustic streaming devices were first introduced in the 1990's. Nature may have preceded this invention by 2.7 Gyr.

1. Outline

Acoustic streaming is the mean (rectified) flow resulting from the attenuation of an acoustic wave. Experimentally demonstrated by Faraday in 1831, a proof-of-concept for microfluidic applications was given in 1991 [39]. There is nowadays a thriving business for microelectromechanical (MEMS) pumps, valves and mixers using *surface acoustic waves* (SAW) [14], [33], [35], [59]. We call attention to the

2000 *Mathematics Subject Classification.* 76Z1, 76C05, 92C17, 74F10
PACS 47.63.Gd, 87.85.gj, 47.61.Fg, 43.25.Nm.
Key words and phrases. acoustic streaming, microswimming, Synechococcus, MEMS devices.
Kurt M. Ehlers, KE acknowledges the support from mathematics and physics faculty at St. Mary's College of Maryland where part of this research was conducted, and to CNPq and Faperj sponsored visits to Rio de Janeiro.
Jair Koiller, JK thanks Fundación Carolina and Centre de Recerca Matematica for a Luis Santaló fellowship, and to CNPq, CAPES and Nehama G.A. for their support.

fact that even in the low Reynolds number regime, there is a contribution from the inertial term of the Navier-Stokes equation.

Filter feeding tunicates seem to rely on acoustic streaming for sensing and food harvesting. It has been suggested that outer hair cells of mammals cochlea have copied (or evolved from) them about 600 million years ago [7]. Atomic force microscopy revealed that many cells generate membrane oscillations at the acoustic range.

1.1. **Results.** We first discuss Lighthill's paper on acoustic streaming in the inner ear [29], as many interesting questions remain open. We take the nerve to present some speculations on the controversial "cochlear amplifier" mechanism.

The main part of this paper is a model for self-propulsion of a microorganism based on acoustic streaming. A good candidate is the cyanobacteria Synechococcus, that swims on open seas without flagella or other visible means of propulsion. We elaborate on two scenarios, announced in a preliminary version `arxiv.org/abs/0903.3781`. In the first, attenuation takes place in the body of the fluid, and the cell is pushed by the resulting flow. While the simplicity of this model is appealing, the power requirement seems too high to be biologically feasible, unless a enhancement mechanism is also present.

The second model employs a traveling SAW. Attenuation takes place in the *Stokes boundary layer* surrounding the cell. Employing this mechanism, a cell the size of Synechococcus can propel itself at observed speeds of 25 diameters per second using an $\omega = 1.5$kHz traveling SAW with wavelength $\lambda = 10^{-5}$ cm and amplitude 10^{-6} cm. If this speculation is confirmed, Nature scooped engineers by 2.7 Gyr.

All things being equal, AS is about 2.5 times more efficient than the "standard model", in which surface tangential deformations interact directly with the incompressible flow Stokes via no-slip boundary conditions. Moreover, acoustic streaming entails a mixing flow in the Stokes boundary layer, and this additional feature is biologically advantageous. For additional biological information we refer to the companion article [22].

1.2. **Traditional microswimming modeling: Aristotelean physics.** According to common wisdom, inertia plays absolutely no role in microswimming. This idea was beautifully explained by Purcell in a lecture given at the 1976 American Physics Society meeeting[45]. However, if Synechococcus use acoustic streaming for propulsion, it will be fair to say that these cells do actually know about Newton's second law[1].

The "textbook rule" is to use the incompressible Stokes equations with noslip boundary conditions, imposing the constraint that a neutrally buoyant, free

[1]We review in Appendix A the traditional approach ([11], [55], [25]). In Appendix B we present the basic theoretical results on acoustic streaming, following Lighthill ([28]. In appendix C we apply the theory for streaming near a vibrating surface.

swimming organism does not exert net forces or torques on the surrounding fluid. This condition holds at each instant of time. As a consequence if the swimmer retraces the stroke in reverse, no matter the time reparametrization, it returns to its initial position ("scallop theorem" or "oyster paradox"). In order to swim at zero Reynolds number an organism or machine must possess at least two degrees of freedom, used in alternate cyclic order. For modern descriptions of this "gauge theory of something" see [52], [21], and for a state of the art review, [25].

In practice, since the 1950's envelope deformation (squirming) models were developed by Taylor and Lighthill, and applied to ciliary propulsion. One solves, quasi-statically, the Stokes equations with no slip boundary conditions given by the instantaneous velocity field defined by the current deformation of a localized shape. To enforce the zero net force and torque one adds a counterflow, given by an infinitesimal translation and rotation. Cyclic but non-reciprocal boundary motions produce a net displacement through the fluid.

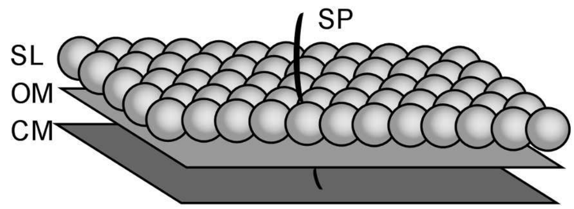

FIGURE 1. Envelope structure of *Synechococcus* consisting of the cytoplasmic membrane (CM), the outer membrane (OM), and the crystalline surface layer (SL). The SL is composed of SwmA arranged in a periodic rhomboidal pattern with 12-nm spacing between individual units [37], [51]. The motile strain WH8113 could be covered with a forest of spicules (SP) [51] while strain WH8102 (also motile) lacks spicules [37].

1.3. **Breaking the paradigm: do cyanobacteria know that "f = ma" ?** Motile strains of the cyanobacteria Synechococcus were discovered in the Atlantic in 1985 [57]. Swimming at speeds of 10-25 diameters per second, their locomotion is unusual in that it does not involve flagella or other structures typically associated with bacterial motility. Both sodium and calcium are required for motility [43]. A glycoprotein, swmA, forms a crystalline surface layer on motile strains. Both swmA and another protein, swmB (which is also localized near the cell surface), are necessary for motility [38]. While photosynthetic as every cyanobacteria, motile strains of Synechococcus do not show a phototactic or photophobic response to light, but do show a chemotactic response to certain nitrogenous compounds. For more biological details, see [22].

We suggest that Synechococcus could be using acoustic streaming for self-propulsion. *We emphasize that this employs an entirely different physical principle than the usual paradigm.* Like the squirming model, small amplitude cyclical motions along the outer membrane are rectified into mean streaming flow, but the difference lies in the underlying physics. In the AS model the membrane oscillations produce a surface acoustic wave. It is the wave-fluid interaction that produces the streaming flow. The inertial term of the Navier-Stokes equations is relevant, as well as the fact that water has some degree of compressibility.

In a symmetric setting, a standing wave generates a mean rotational flow near the membrane which for instance can be used for enhancing nutrient uptake. In an asymmetric geometry, even a standing (hence reversible) wave could produce locomotion, in flagrant violation of the scallop theorem.

2. Acoustic streaming and piezoelectricity in cell biology

Although there is just a note on the subject in his celebrated 1877 *Theory of Sound* [46], a few years later Lord Rayleigh provided a theoretical foundation for acoustic streaming, in an analysis of Kundt's tubes [47]. Rayleigh wrote also an important paper on solid/fluid interactions [48]. After a long period of dormancy, Nyborg (and others) revived acoustic streaming in the 1950's, motivated by the emerging area of medical ultrasound (see [60] for a recent review article).

Also around 1880 properties of piezoelectric crystals where being studied by Pierre Curie and his older brother Jacques Curie. Piezoelectric materials convert mechanical deformations into voltage differences, and vice versa, providing a wonderful form of energy transduction. The piezolectric effect was regarded as a curiosity at that time. Nowadays, its applications range from door buzzers, microphones and electric guitar pick-ups, to auto-focus cameras, sensors in cars, aeronautical and space instrumentation, and is fast moving into nanotechnology.

2.1. **Physics of acoustic streaming.** Acoustic streaming is a subtle nonlinear, second order effect. As we mentioned before, in traditional microswimming modeling, water is assumed to be incompressible, but AS takes into account that it has some degree of compressibility. Even for highly viscous flows part of the inertial term in the Navier-Stokes equation must be retained. It is the *attenuation* of sound, due to viscosity, that creates a gradient in the momentum flux, producing a steaming flow.

In his 1978 review [27] Lighthill describes the theory of acoustic streaming in both low and high Reynolds number regimes. Later, Riley presented a somewhat broader view called *steady streaming* [50]. The low Reynolds number situation, which is appropriate for our purposes, is called *RNW streaming* after Rayleigh, Nyborg and Westervelt.

The attenuation necessary for streaming can occur in the body of the fluid or in a *Stokes boundary layer* surrounding a surface. Acoustic streaming due to attenuation in the body of the fluid can be observed when a quartz crystal is electrically excited, producing high frequency vibrations. This is commonly called a *quartz wind* (QW). In air, jets with speeds of up to 10cm/sec can be generated in front of the face of a quartz crystal excited with an electrical current. In Lighthill's words, "not only can a jet generate sound, but also sound can generate a jet". The QW effect is generally associated with high power sources of ultrasonic acoustic energy.

The second form of AS occurs near boundaries. Here the attenuation of the sound wave is a result of strong shear stresses within the Stokes boundary layer. If $\mathbf{U}$ is an oscillating velocity field in a fluid then this layer is the region surrounding the surface where the bulk flow vorticity is non-zero; the streaming flow is irrotational outside this layer. The effective thickness of the Stokes boundary layer is $5(\nu/\omega)^{1/2}$ where ν is the kinematic viscosity and ω is the frequency of $\mathbf{U}$. Boundary induced streaming can be generated either by a acoustic wave in the fluid or vibrations of the boundary itself; the streaming is a result of relative motion.

Summarizing: outside the Stokes layer flow is laminar, irrotational. Within the Stokes layer, the flow is turbulent, rotational. We can poetically imagine a chaotic "fluid atmosphere" surrounding the cell. Our calculations indicate that, surprisingly, the Stokes layer is non-negligible.

2.2. **Possible acoustic streaming instantiations in cell biology.** Acoustic streaming MEMS systems are nowadays a standard tool for bioassays: fluids can be easily pumped or mixed in the microscale.

Therefore, Nature must have taken advantage of acoustic streaming. However, as far as we know, the only situation for which AS has been explicitly proposed is in Lighthill's cochlear model.

Three recent cell biology findings were eye-opening to us:

(1) In [37] and [51], deep-freeze electron microscopy of the motile Synechococcus strains 8102 and 8113 revealed the presence of a crystalline outer "S-layer . In the latter, a forest of "spicules" was also observed, extending from the inner membrane, and projecting 150 nm into the surrounding fluid[2]. In the former, mutant cells lacking the outer S-layer, composed of swmA, do not swim (when accidentally attached to a slide, however, they still rotate).

(2) Using atomic force microscopy (AFM), the outer membranes of Yeast cells have been observed to oscillate at between 0.8-1.6 KHz with typical amplitudes of $\sim$ 3nm [41]. The oscillations were shown to be driven by

[2]There are some doubts if the spicules could have been artifacts of preparation. They are not necessary to our model, but are helpful.

molecular motors[3]. The magnitude of the forces at the cell wall were measured to be $\sim$10nN suggesting that they are generated by many protein motors working cooperatively.

(3) In [44], quantitative phase imaging (QFI) was used to detect nanoscale vibrations of the order of 200 nm in red blood cells.

We could also add diatoms to this list. These organisms come up after cyanobacteria in the tree of life. Diatoms are very popular among bioengineers, since they are basically of the same size, shape and material as microchips (and very cheap to produce - the ideal template). We speculate that they could use acoustic streaming to pump fluid along their raphe, a microchannel in their crystalline surface. For basic information, see [10] and the special issue on diatom nanotechnology [16].

3. Lighthill's cochlear model and its possible developments

Sir James Lighthill has suggested that acoustic streaming may play a role in mammalian hearing [29]. Localized oscillations of the basilar membrane within the fluid filled cochlea would lead to acoustic streaming induced motions, sufficient to deflect the stereocilia of the inner hair cells of the cochlea (when the stereocilia are deflected an electric signal encoding the sound wave is sent to the brain).

3.1. **Physiology: outer and inner ear structures.** Sound waves collected by the auricle at the outer ear pass through the auditory canal striking the tympanic membrane (eardrum). The sound wave is then transmitted through the middle ear through the ossicles consisting of three delicate bones: the hammer that is in contact with the tympanic membrane, the anvil, and the stirrup which is in contact with the oval window of the cochlea.

Vibrations of the stirrup on the oval window cause a traveling wave within the fluids of the cochlea. Within the cochlea sounds are decomposed into their component frequencies, converted into an electrical signal and transmitted to the brain. The cochlea is shaped like the shell of a snail with 2 1/2 turns, and consists of three fluid filled sections: the scala vestibuli, the scala tympani and the scala media. The scala vestibuli and scala tympani are filled with a fluid called perilymph and are connected at the apex of the cochlea. The scala media is partitioned from the scala vestibuli by the Reissner's membrane and from the scala tympani by the basilar membrane and is filled with a fluid called endolymph with a high concentration of positively charged potassium ions. Sitting atop the basilar membrane is the organ of corti which converts the mechanical sound wave into an electrical signal.

[3]Since the 1970's, power source systems have been identified for intracellular transport (kinesin molecular motors), locomotion systems for bacteria (protonmotive rotary motors), and protozoa (dynein motors distributed along the axonemes).

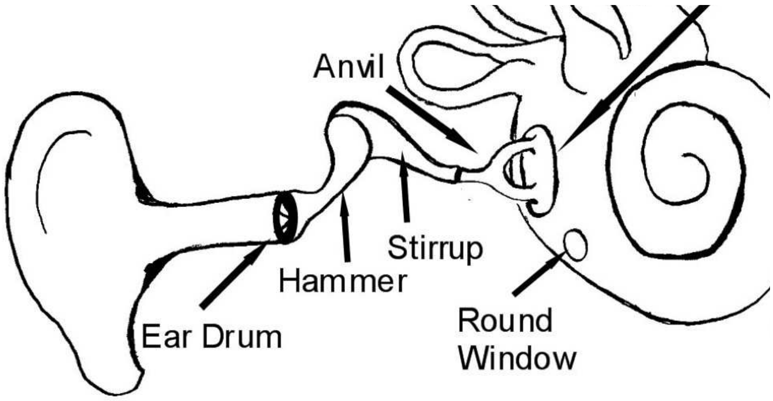

FIGURE 2. The basic layout of the human ear. Sound waves transmitted through the bone of the middle ear enter the cochlea through the oval window. The membrane of the round window moves in the opposite direction of that of the oval window and is necessary because of the incompressibility of the cochlear fluids.

The key to the ability of the ear to decompose frequencies is the structure of the basilar membrane. Each position along its length is tuned to a particular frequency. Near the oval window it is narrow and stiff being tuned to high frequencies. Near the apex of the cochlear duct it is tuned to low frequencies being wide and compliant. The stiffness decreases by four orders of magnitude from the base to the apex. The basilar membrane is constructed of radial fibers allowing a particular place to oscillate nearly independently of nearby places.

The organ of Corti has two type of hair cell: outer hair cells (involved with the cochlear amplifier) and inner hair cells. The inner hair cells of the organ of Corti act as sensory receptors. Each hair cell has approximately 300 "hairs" called stereocilia. A hair cell normally carries a voltage potential across its outer membrane but if the stereocilia are deflected, positive ions are allowed to enter causing depolarization of the cell. This sets off a chain of events resulting in an electric signal being sent to the brain.

A great deal of biological information has been obtained recently [3], motivating a boom of theoretical work, with very different approaches. In what follows we admittedly go very bare.

3.2. **Lighthill's model: acoustic streaming in the cochlea.** Sound waves transmitted to the cochlea induce a traveling wave along the basilar membrane. As the traveling wave approaches the characteristic place for the particular frequency ω its phase speed c slows, its spatial wavelength $\lambda = 2\pi c/\omega$ shrinks, its amplitude V increases to a peak. Then precipitously drops. The wave energy per unit length E reaches a maximum $E^{\max}$ at the characteristic place.

Mammals have evolved a remarkable cochlear amplifier that both increases the amplitude at the characteristic place and sharpens the peak [3]. Amplification, which is between 20 and 30 decibels, results from motility of the outer hair cells of

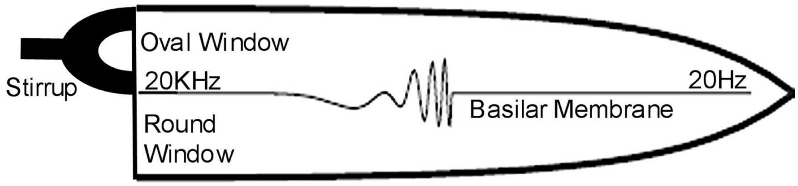

FIGURE 3. Simplified diagram of an uncoiled cochlea. Characteristic places for high frequencies are near the base of the cochlea and characteristic places for low frequencies are near the apex. Sound waves entering the the cochlea induce a traveling wave along the basilar membrane. The wave speed slows dramatically at the characteristic place for the frequency. The spatial wavelength shortens and the amplitude increases to a peak then falls off precipitously.

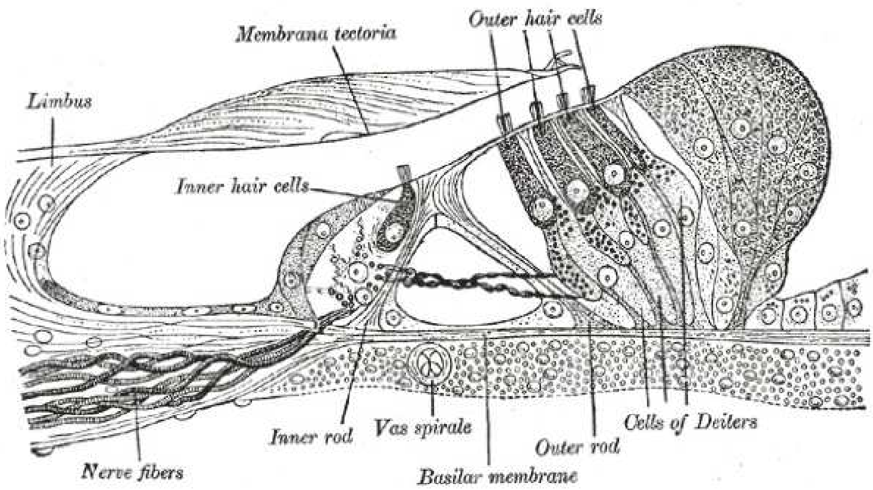

FIGURE 4. The Organ of Corti (Gray's anatomy classical figure). The inner hair cells are responsible for converting the mechanical action of a sound wave to an electrical signal. The outer hair cells are involved in the mammalian cochlear amplifier.

the organ of Corti in response to a positive feedback control system, whose precise workings in the subject of intense debate. The fact is that cochlear amplifier allows mammals hear nuances of speech and music over a wide dynamic range of intensity.

While the hairs of the outer hair cells are deflected by direct contact with the tectorial membrane (see figure 4) inner hair cells are deflected by motions of the endolymph itself. This is where acoustic streaming could play a role. In his 1992 paper *Acoustic streaming in the ear itself* [29] Lighthill shows that significant acoustic streaming with velocity

$$\frac{1}{4}V^2c^{-1} - \frac{3}{4}V(dV/dx)\omega^{-1} \tag{1}$$

occurs near the characteristic place. Here $(V(x), 0, 0)$ is the velocity amplitude of the basilar membrane's vibration. Recall that at the characteristic place the phase speed c rapidly diminishes to zero while the velocity amplitude increases greatly enhancing the streaming velocity. Lighthill uses this result to obtain the estimate for the volume outflow per unit length along the basilar membrane

$$\frac{0.015E^{\max}}{\rho L\sqrt{\omega\nu}} \tag{2}$$

where ρ is the density and ν is the kinematic viscosity of the endolymph (these are essentially those of pure water). L is the e-folding distance of the stiffness of the basilar membrane or the distance over which the stiffness decreases by $1/e$=37% of its original value (approximately 6-7mm for a human cochlea). If the cross sectional geometry of the scala media causes the flow q to be channelled between the organ of Corti and the tectorial membrane, the stereocilia of the outer hair cells could be also deflected by the throughflow.

3.3. **Open questions.** Lighthill, who died in 1998 while swimming around the island of Sark (one of his favorite past times), did not publish his planned sequel. Several important open questions are:

- Is the streaming q channelled through the space between the tectorial membrane and the inner hair cells?
- If so, what is the resulting force exerted on the stereocilia?
- How is streaming enhanced by the action of the outer hair cells?

The first question seems to have been answered positively, see [4]. Fluid mediated communication between inner and outer hair cells may ocurr also in the Corti tunnel, see [20].

We finish this section outlining one possibility for a positive feedback loop. We do not claim originality nor correctness, as the "grand picture" for the cochlear amplifier mechanism is in order.

(1) External sound waves enter the oval window. Acoustic streaming along certain places of the basilar membranes set endolymph fluid motion.
(2) This motion induces deflections of the inner hair cells stereocilia opening channels that trigger electric signals to the brain, but also to the outer hair cells.
(3) As the outer hair cells receive these signals, prestin is activated, making the cells oscillate up and down.
(4) These oscillations deflect the outer hair cells stereocilia. The channel flow (called q) is enhanced, again by acoustic streaming, or via the tectorial membrane motion. We get more endolymph fluid motion.
(5) This enhanced endolymph fluid motion enters in loop with step 1.

4. Acoustic streaming in microswimming

We now turn to the main part of the paper. We begin with an estimate of the streaming velocity associated with the oscillatory motion of a yeast cell, using the parameters found by Pelling [41]. According to Rayleigh's classical result, for a standing wave with velocity $U(x)e^{i\omega t}$, the local streaming is given by (see appendix A for a discussion of this formula)

$$U_L = -\frac{3}{4\omega}U(x)U'(x). \tag{3}$$

We take

$$U(x) = 0.003(1500\pi)\sin(2\pi x) \tag{4}$$

corresponding to a 1.5kHz vibration with a 3nm amplitude. We have (arbitrarily) taken the spatial wavelength to be one micron. The streaming velocity is approximately

$$-0.1\sin(2x)\mu m/sec. \tag{5}$$

We note that the streaming velocity is directed away from the antinodes and towards the nodes and is not propulsive. Nonetheless, the rotational streaming velocities in the fluid near the cell membrane should enhance cell chemistry through local mixing.

We now present two scenarios for locomotion involving acoustic streaming. The first one has, in fact, been used for propelling an experimental underwater vehicle[4], but it is not efficient in the low Reynolds regime. The second scenario, on the other hand, is quite competitive, as we now report.

4.1. **Quartz wind model.**

In this simplest model, attenuation of the acoustic beam in the bulk of the fluid generates a flow, pushing the organism through the fluid[5].

Here is a "back of the envelope" computation: Stokes' law $F = 6\pi\mu av$ gives the force required to push a sphere of radius a through a fluid with viscosity μ at speed v. Lighthill [28] argues that the force (F) is related to the acoustic power (P) and the speed of sound in the fluid (c) by

$$F = P/c. \tag{6}$$

The necessary acoustic power is then

$$P = 6\pi\mu avc. \tag{7}$$

Synechococcus has a radius of about 10^{-4}cm and swims in sea water (viscosity 10^{-2}g/cm sec) at about 2.5×10^{-3}cm/sec. It would therefore require about 7×10^{-10} watts of acoustic power to drive Synechococcus at observed speeds.

[4] `http://censam.mit.edu/news/posters/hover/1.pdf`

[5] We wonder of spicules could also help, by pushing and pulling the S-layer in the manner of the Brazilian samba instrument known as "cuica", consisting of a drum with a short bamboo reed penetrating its head.

By comparison, the power needed to push the cell is $6\pi\mu a v^2$ or approximately 1.18×10^{-17} watts. Lighthill [26] defines an *efficiency* η for a swimming mechanism as the ratio of the power required to push the cell to the power required by the mechanism:

$$\eta = 6\pi\mu a v^2/P. \tag{8}$$

By this definition, the efficiency of the quartz wind mechanism is only about

$$1.7\times10^{-6}. \tag{9}$$

The acoustic power necessary for an organism to swim using this mechanism might be unrealistically high. In the discussion we speculate on possible power output enhancement mechanisms.

4.2. **Boundary induced streaming: surface acoustic waves.** In this model a high frequency traveling SAW passes along the crystalline outer S-layer of the cell leading to boundary induced streaming. The vibration is (literally!) piezoelectrically transduced by molecular motors. Spicules, if present, help attenuation and/or to provide sound guidance. The progressive acoustic wave induces a steady slip-velocity at the outer edge of the Stokes boundary layer.

We found that Lighthill's efficiency for boundary induced streaming approaches 1%, comparing favorably with the squirming and flagellar propulsion strategies. The amplitude of the SAW necessary to drive an organism the size of Synechococcus at observed speeds is on the order of 10^{-7}cm, too small to be resolved using light microscopy.

In order to estimate the velocity and efficiency for a spherical cell that swims using a traveling SAW, for simplicity we consider a tangential SAW (though a normal SAW would also lead to self-propulsion). We compute the streaming velocity and the power (per unit area) for a swimming slab, then use these results to estimate the swimming velocity and power output for a spherical organism. The "tangent plane approximation" was proposed in [52] for estimates in the traditional microswimming approach. It provides a good estimate when the wavelength of the SAW is much smaller than the radius of the cell.

Consider a slab of infinite extent with coordinates (x, y) bounding an infinite region of water in the region $z \geq 0$. Suppose tangential progressive waves pass along the slab in the $+x$-direction with

$$x_m = x + A\sin(nx - \omega t) \tag{10}$$

where x_m is a material line on the slab.

The streaming velocity just outside the Stokes layer is then $U = -A\omega\cos(nx - \omega t)$. The streaming velocity at the edge of the Stokes layer is then

$$U_L = -\frac{5\pi}{2\lambda}\omega A^2 \tag{11}$$

where $\lambda = 2\pi/n$ is the wavelength (see appendix A for a derivation of this formula).

Now consider a spherical organism of radius r that swims by passing high frequency traveling compression waves along its outer membrane. Let (θ, ϕ) be spherical coordinates with ϕ the azimuthal coordinate measured from the front of the organism. Take the wave to be

$$\phi_m = \phi + \epsilon \sin(n\phi - \omega t) \tag{12}$$

where ϕ_m represents a material point on the outer membrane. The amplitude of the of the velocity is $A = \epsilon r \omega$ and the wavelength is $\lambda = 2\pi r/n$. We assume that $\lambda << r$ so that the local streaming velocity is well approximated by (11). In this case, we take as a slip-velocity

$$\mathbf{U} = \frac{5}{4} n \omega \epsilon^2 \mathbf{i}_\phi \tag{13}$$

where $\mathbf{i}_\phi$ is the unit vector in the direction of the azimuthal spherical coordinate at the surface of the cell.

A convenient formula for the translational velocity associated with any boundary velocity field was derived using the Lorentz reciprocity theorem in [12], [55], which, for a sphere is

$$\mathbf{V} = \mathbf{A}(\mathbf{U}) = -\frac{\mathbf{1}}{\mathbf{4\pi r^2}} \int\int_{\mathbf{S}} \mathbf{U}\, \mathbf{dS} \tag{14}$$

where the integral is taken over the surface of the sphere. Evaluating this with velocity (13) we find that the spherical organism swims with velocity

$$\frac{5}{16} \pi n r \omega \epsilon^2 \tag{15}$$

along the axis of symmetry. Note that the amplitude of the SAW is $r\epsilon$ and $\omega = 2\pi f$ where f is measured in Hertz. Written in terms of wavelength and phase velocity of the traveling wave $c = \lambda \nu$ this velocity can be written

$$(5\pi^3/4)(\epsilon/\lambda)^2 c \tag{16}$$

This is 2.5 times the velocity predicted by the squirming mechanism all parameters being equal [11].

4.3. **Efficiency of the SAW mechanism.** To estimate the effort required to execute the compression waves we compute the power

$$P = \int\int_S v_i \sigma_{ij} dS_j \tag{17}$$

averaged over a swimming stroke. Again we assume $\lambda << a$ and approximate the average power using the average power per unit area for a waving sheet. For a sheet in the xy-plane with a fluid of viscosity μ filling the region $z \geq 0$, the average power per unit area necessary to deform according to

$$x_m = x + A \sin(kx - \omega t) \tag{18}$$

TABLE 1. Possible AS parameters in the biological range

Frequency (Hz)	Amplitude (cm)	Wave Speed (cm/sec)	Power (Watts)	η (%)	Stokes layer (cm)
500	1.64×10^{-6}	0.01	1×10^{-15}	1.17	1.78×10^{-3}
1000	1.16×10^{-6}	0.02	2×10^{-15}	0.59	1.26×10^{-3}
1500	9.49×10^{-7}	0.03	3×10^{-15}	0.39	1.00×10^{-3}
5000	5.20×10^{-7}	0.10	1×10^{-14}	0.12	3.99×10^{-3}

is

$$2\pi\mu\omega^2 A^2/\lambda \tag{19}$$

where $\lambda = 2\pi/k$, see [8]. For the sphere deforming according to (12) we have $A = r\epsilon$ and $\lambda = 2\pi r/k$. Substituting these into (19) and multiplying by the area we arrive at

$$P = 4\pi\mu r^3 n\omega^2\epsilon^2. \tag{20}$$

We note that this expression is in good agreement with the result obtained by evaluating (17) in spherical coordinates for large n; for instance, when $n = 10$ the actual coefficient is 4.04.

The power output and efficiency for a cell of radius 10^{-4} using boundary induced acoustic streaming to swim at 2.5×10^{-3}, the observed speed of Synechococcus, is given in table 1 where we have (arbitrarily) chosen $n = 30$.

5. Discussion

The quartz wind strategy is less efficient by many orders of magnitude and is probably not biologically feasible unless some mechanism for power enhancement is present. On the other hand, all things being equal, propulsion by surface acoustic waves predicts a swimming velocity 2.5 times that predicted by squirming.

For Synechococcus, the required frequency of the SAW is within the range observed in other biological systems. The amplitude required for observed speeds is on the order of 10^{-6} cm, below the resolution limit of light microscopy. This leads to the key question. If acoustic streaming generated by surface acoustic waves is responsible for the locomotion of Synechococcus, how could we "listen to their songs"?

5.1. **Experiments.**

We refer to the companion paper [22] for recent biological findings. The "holy grail" is identifying the molecular motor. A theoretical model for how cells can generate high frequency oscillations using coupled molecular motors has been developed by Jülicher [19], predicting that molecular motors working in unison can produce cellular oscillations with frequencies of 10KHz and beyond.

Prestin, the outer hair cell molecular motor was identified in 2000, functions like piezoelectric transducer. Will a similar molecular motor be found for Synechococcus? (Gliding cyanobacteria contain a glycoprotein, *oscillin*, which has some homology to swmA, but both seem to have a passive role in locomotion.) Here we suggest some physical experiments based on recent developments in nanotechnology.
AS nanosensors: listening to the sound of cells. Can one "hear" the sound generated by a moving Synechococcus, via nanosensors attached to the crystalline shell? Cantilever/nanowire devices are already available that can measure piezoelectric displacement transduction whose frequency and amplitude approach the quantum regime.

Pelling, et. al measured periodic oscillations with amplitudes of 3nm at frequencies of 0.8-1.6kHz on the of the outer membrane of Yeast cells using the cantilever of an atomic force microscope [41]. Living Yeast cells that measure about 5μm in diameter were trapped in the micro-pores of a filter for the experiment. Yeast cells were chosen for the experiment due to their stiff cell wall; the spring constant of the cantilever needs to be comparable to the spring constant of the cells wall. Could this experiment be adapted to "listen" a Synechococcus? For the state of the art on AS sensors at the microscopic realm we refer to a recent review paper [31].
Direct visualization/manipulation of the flow. We believe it possible to map the flow pattern of the fluid adjacent to a swimming cell using technologies such as total internal reflection velocimetry (TIRV, see the review [17]). There are no technological limitations anymore. By 2011 it is expected that particles of 25 nm will be able to be manipulated on chips, see International Technology Roadmap for Semiconductors $http://www.itrs.net/$.

The observed flow via TIRV could be matched with the characteristics of acoustic streaming induced flow. Detailed analysis of the fluid mechanics and careful experimentation would be required in the case of a progressive (propulsive) SAW. A very interesting and challenging mathematical problem is to model the chaotic flow pattern inside the "atmosphere" (the Stokes layer) surrounding the cell. Note that our estimates showed that it is non negligible[6]

We note that experiments on diatoms should be simpler to do. Fluorescent beads inside the raphe could be focused by a standing SAW. Certainly some of the techniques of described in [31] could be applied to a diatom skeleton to probe its piezo/mechanical properties.

[6]Prof. Howard Berg (personal communications) tried to visualize the flow with particles under common microscopy, but there was "too much Brownian motion". Could that be in fact a signature of the chaotic near boundary flow?. Marker patterns in flows generated by biflagellated algae cells have been just recently observed and can be seen in $http://www.haverford.edu/physics/Gollub/SwimminMicroorganisms/$ and in arxiA 0910.1143v1.

5.2. **Related effects.**
Quartz wind enhancement: uasers. Quartz wind is a very simple mechanism, but it is inefficient in the low Reynolds regime. One way to remedy this drawback is to imagine a power enhancement mechanism similar to a laser. *Uasers* [58] are coupled ultrasonic transducers producing stimulated emission via positive feedback with an internal power mechanism. Power output scales with the square of the number of oscillators, and one could try to find signs of phase locked excitations (a samba school "cuica" orchestra).
Streaming flow enhancement by submicrobubbles. Nyborg pointed out, many years ago, that an external ultrasound source resonating immersed bubbles adjacent to a cell could induce internal cellular processes. Conversely, acoustic waves produced by the cell could resonate submicrobubbles attracted to the crystalline layer, enhancing the streaming flows. Experiments with inorganic materials have confirmed this effect [35].
Cavitation energy. Lord Rayleigh has already studied the deleterious effects of cavitation on ship propellers. In medical ultrasound it must be taken care off, but it may also be used to perform microsurgeries or to insert biological materials on cells. One could speculate on a locomotion model based on direct extraction of energy stored in submicrobubbles, perhaps coupled to some ratchet type mechanism. Moreover, in the process of bubble collapse, several chemical reactions occur [9]. A curious coincidence is that chemical reactions involving nitrogenous compounds are commonly produced in bubble cavitation. This may be of interest since Synechococcus is attracted to nitrogen.
Hydrophylic/hydrophobic transitions. Micro-engineered surfaces coated with nanonails, when charged, exhibit controlled hydrophylic-hydrophobic transitions [1]. One can speculate that an hydrophylic-hydrophobic wave could entrain pumping motion, mediated perhaps by some ratchet type asymmetry or bubble manipulation. This is another suggestive clue, since the spicules project 0.15 μm to the exterior of the crystalline shell. Devices with chemically induced hydrophylic-hydrophobic microtracks have been recently constructed [49],[59].

5.3. **Mathematical remarks and possible developments.** A somewhat simpler but nonetheless intriguing viewpoint has been proposed in [53]. In order to estimate the streaming flow inside a spherical cavity, "vorticity boundary conditions" were applied directly to the incompressible Stokes equations. In our setting, one would consider the external flow.

In a similar vein, the "blinking stokeslets" proposed by Blake and coworkers [5] can be reinterpreted as true "physical" generators of the acoustic wave. This appeoach is appealing as it connects directly with the membrane force generators.

In another tack, we call attention to recent theoretical and computational developments by Wixforth's group, motivated by surface acoustic waves on microchips [2], [15], [23], [24]. They derive the PDEs coupling the piezoelectric effect with the Navier-Stokes equations from *ab-initio* considerations. It would be interesting to apply these techniques to our setting, when enough biological information becomes available.

5.4. **Conclusion.** In a recent review [54] MEMS devices physical processes are classified into three main types: A. *Electrokinetic*, B. *Steady streaming*, and C. *Direct fluid structure interactions.*

Type A mechanisms such as electrophoresis have been ruled out for Synechococcus [42]. Any motions of the cell's outer membrane are small enough that they are undetectable by light microscopy whose resolution limit is about 200 nm. Compression-expansion tangential waves along the membrane (a subtle type of squirming), a type C mechanism, was proposed in the mid 90's [11], [55].

In this article we proposed instead a type B mechanism: *free to move in a fluid a "singing" microorganism or robot would swim rather than pump.* Acoustic streaming is not just one more way of moving. It has been known since the fundamental work by Nyborg [40] that local mixing near the boundary is enhanced by AS. Experimental literature confirmed that AS enhances local mixing [33], [56], and commercial microfluidic mixers are available nowadays.

In [34] the average mass transfer available to a spherical "squirming swimmer" (using tangential surface waves) is estimated. An important parameter here is the Péclet number, governing the ratio between advection to diffusion. It would be interesting to compare this with estimates of mass transfer and mixing coming from acoustic streaming. Perhaps some controlled laboratory experiment could be devised using chemo-attractants that would react near a Synechococcus.

With techniques such as AFM and QFI to detect cell vibrations and total internal reflection microscopy for micro-fluidic visualization, we believe the time is ripe to solve the Synechococcus mysterious motility. The results of Pelling [41] indicate that cell oscillations with frequencies that lead to AS are feasible. Pelling has noted that the sound produced by yeast cells may be an indication of a pumping system that supplements passive diffusion. We suggest that *sound itself is the pumping mechanism.* Synechococcus would swim while singing.

This year marks the 50th anniversary of Richard Feynman's famous Christmas talk at Caltech [13]. We think that he would like the idea of biological "samba loudspeakers". He was fond of Brazilian carnival, in particular the "cuica".

Acknowledgements

This article is an outgrowth of a talk given at IMPA's Workshop Mathematical Methods and Modeling of Biophysical Phenomena Angra dos Reis, Rio de Janeiro, 2009. We thank Howard Berg, Jay McCarren, Richard Montgomery, John Bush, Steve Childress, Moyses Nussenzweig, Sandra Azevedo, for many informations and questions raised in the preparation of the manuscript.

Appendix A. Swimming at low Reynolds number: traditional view

In this appendix we review the kinematics of swimming at low Reynolds number. For an informal discussion see the classic paper of Purcell [45] and for more details [21], [25], [52].

For a swimming microorganism the appropriate equations of motion are the incompressible Stokes equations

$$\mu \Delta \mathbf{v} = \nabla \mathbf{p} \quad , \quad \nabla \cdot \mathbf{v} = \mathbf{0} \tag{21}$$

which are to be satisfied at each instant on the fluid domain exterior to the cell. Here $\mathbf{v} = (\mathbf{v_1}, \mathbf{v_2}, \mathbf{v_3})$ is the Eulerian velocity field, p is the corresponding pressure, and μ is the viscosity. (Note that the viscosity (μ) is related to the kinematic viscosity ν by $\mu = \rho\nu$ where ρ is the density of the fluid.) The boundary conditions are no-slip meaning that the fluid velocity immediately adjacent to the cell membrane matches the instantaneous velocity of the cell membrane. The fluid velocity is assumed to vanish at infinity.

Let Σ represent the (located) outer membrane of the cell (or the edge of the Stokes boundary layer) and let $\mathbf{V}$ be a vector field on Σ representing an infinitesimal boundary deformation. The net force and torque exerted on the fluid is then

$$\mathbf{F} = -\int_{\Sigma} \sigma(\mathbf{V}) \cdot \mathbf{ndS} = \mathbf{0} \tag{22}$$

$$\mathbf{T} = -\int_{\Sigma} (x_1, x_2, x_3) \times \sigma(\mathbf{V}) \cdot \mathbf{ndS} = \mathbf{0} \tag{23}$$

where σ is the stress tensor. The basic principal of low Reynolds number swimming is that a free swimming microorganism does not exert net forces or torques on the surrounding fluid. Associated with $\mathbf{V}$ there is a corresponding rigid translation and rotation of Σ necessary to cancel any net force or torque. This assignment is linear and defines a linear map

$$A_\Sigma : T\Sigma \to se(3)$$

where $T\Sigma$ is the set of vector fields on Σ and $se(3)$ is the algebra of infinitesimal Euclidean motions of $\mathbf{R}^3$. The corrected force and torque free vector field is thus $\mathbf{V} - \mathbf{A_\Sigma}(\mathbf{V})$.

Useful formulas for the translational and rotational components of A for a sphere were derived using the Lorentz reciprocity theorem in [55]:

$$A^{\text{tr}} = -\frac{1}{4\pi r^2} \int\int_S \mathbf{U}\, dS \quad \text{and} \quad A^{\text{rot}} = -\frac{3}{8\pi r^3} \int\int_S \mathbf{n} \times \mathbf{U}\, \mathbf{dS} \tag{24}$$

where the integral is taken over the surface of the sphere.

If $\Sigma(t)$, $0 \leq t \leq \tau$ represents a cyclic swimming stroke with $\Sigma(\tau) = \Sigma(0)$ then the net rigid motion is given by the path ordered exponential

$$g = \overline{P}exp\left(\int_0^{\tau} A_{\Sigma(t)}(\Sigma'(t))dt\right) \in SE(3) \tag{25}$$

where $\Sigma'(t)$ is the vector field representing the infinitesimal boundary deformation at t and $SE(3)$ is the group of Euclidean motions.

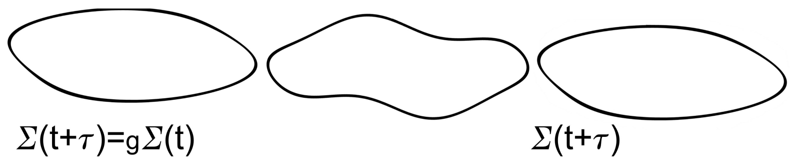

FIGURE 5. After a cyclic but nonreciprocal swimming stroke the swimmer returns to its original shape but is displaced by a Euclidean motion $g = g = \overline{P}exp\left(\int_t^{t+\tau} A_{\Sigma(t)}(\Sigma'(t))dt\right)$

This integral can computed explicitly for large boundary deformations only in rare cases (see [52] for an example) but can be approximated to second order in the amplitude in many important cases. These approximations are useful since many Stokesian swimmers propel themselves using high frequency small amplitude boundary undulations (many ciliates, for example, are effectively modeled as squirming spheroids, see [26], [5]).

In [11] (see also [55]) a mechanism involving progressive compression waves along the outer membrane was proposed for Synechococcus. If the axially symmetric compression waves have amplitude a and wavelength λ, and c is the wave speed, then the swimming velocity is

$$V_{\text{squirming}} = \left(\frac{\pi^3}{2}\right)\left(\frac{a}{\lambda}\right)^2 c\ . \tag{26}$$

APPENDIX B. ACOUSTIC STREAMING

Acoustic streaming is the mean flow in a fluid generated by the attenuation of an acoustic wave. The basic theory was developed by Lord Rayleigh in the late 19th Century. Modern accounts, which we follow in this brief description of the theory, can be found in [40], [27], [50]. In this appendix we review the basic principles of acoustic streaming following Lighthill's formulation. He emphasizes that streaming is the result of a gradient in the *Reynold's stress*, which is the mean value of the acoustic momentum flux, caused by attenuation of the sound energy.

To describe the force driving the mean flow associated with an acoustic field we let (x_1, x_2, x_3) be coordinates on $\mathbf{R}^3$ representing the fluid domain and $\mathbf{u} = (u_1, u_2, u_3)$ represent the oscillatory particle velocity. The momentum, per unit volume is then $\rho\mathbf{u}$ where ρ is the fluid density. The momentum vector at a point is carried by the flow of $\mathbf{u}$ so we can speak of momentum flux across a surface. The flux per unit area of the i-component of the momentum vector in the x_j-direction is $u_j(\rho u_i)$. The Reynolds stress tensor is then $\overline{\rho u_i u_j}$ where the bar indicates the mean taken over many cycles. The Reynolds stress, representing mean momentum flux is a force per unit area directed in the x_j-direction.

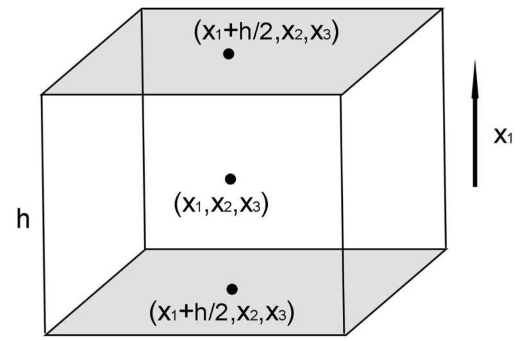

FIGURE 6. Element of fluid acted upon by Reynolds stress.

In figure 5 he x_1-component of the per unit volume associated with the component $\overline{\rho u_i u_1}$ of the stress on the small fluid box with dimension h centered at (x_1, x_2, x_3) is the difference between the forces on the shaded sides, or

$$\frac{1}{h^3}(-h^2\overline{\rho u_i u_j}|_{(x_1+h/2,x_2,x_3)} + h^2\overline{\rho u_i u_j}|_{(x_1-h/2,x_2,x_3)}). \tag{27}$$

Letting $h \to 0$, the force per unit volume for this component of the stress is $-\partial/\partial x_1(\overline{\rho u_i u_1})$ and the total force is found by summing over i. In general, the force driving the mean streaming motion is $\mathbf{F}$ where

$$F_j = -\sum_i \partial/\partial x_j(\overline{\rho u_i u_j}) \tag{28}$$

which is nonzero if there is some mechanism for attenuation of the sound wave. Without attenuation the gradient is zero and there is no mean forcing. We note that (28) is equivalent to

$$\mathbf{F} = -\rho(\overline{\mathbf{u}\cdot\nabla\mathbf{u} + \mathbf{u}\nabla\cdot\mathbf{u}}) \tag{29}$$

used by Nyborg [40].

Two mechanisms for sound attenuation give rise to two primary forms of acoustic streaming: *quartz wind* and *boundary induced streaming.* With quartz wind the attenuation is a result of shear stresses in the body of the fluid. This effect can be observed in the laboratory when a quartz crystal is electrically excited producing strong ultrasonic beams off its faces into the surrounding air producing turbulent jets with velocities on the order of $10cm/sec$. The quartz wind requires high acoustic power and high frequency for significant streaming velocities.

In boundary induced streaming the attenuation occurs in the layer of fluid (the Stokes layer) just outside a solid wall. Because of the strong shear stresses within this layer attenuation is much greater and significant streaming occurs at lower frequencies and powers. Boundary induced streaming is the principle behind the common science museums device known as a Kundt's tube. A standing acoustic wave is established within a hollow tube containing fine dust. The dust accumulates at the antinodes of the standing wave, allowing the relationship between the frequency, wavelength, and sound speed to be measured.

Appendix C. Progressive acoustic wave near an oscillating wall

We now show that a progressive acoustic wave transverse to a solid boundary leadsto a steady streaming velocity in the direction of the wave, just outside the Stokes layer. The streaming is a result of the relative motion of the fluid and streaming can result from either sound waves in the fluid or oscillations of the solid boundary. We use Lighthill's formulation to compute the streaming velocity associated with a traveling acoustic wave directed in the $+x$-direction in a fluid in the region $z > 0$ bounded by a solid wall at $z = 0$. Let u and v be the x and y components of the fluid velocity. We assume the y component of the velocity is zero.

Suppose the amplitude of the traveling wave in the body of the fluid far from the wall is given by the real part[7] of

$$U \exp(i(nx + \omega t)) \tag{30}$$

Momentum in the fluid diffuses with diffusivity $\nu = \mu/\rho$ and the effect of the no-slip condition at the wall on the otherwise oscillating fluid diffuses according to $e^{-z\sqrt{i\omega/\nu}}$. Justification of this statement can be found in [27, section 2.7]. The x component of the fluid velocity is thus

$$u = U \exp(i(nx + \omega t))(1 - e^{-z\sqrt{i\omega/\nu}}). \tag{31}$$

The Stokes layer is that region adjacent to the wall where the flow is rotational. In figure (C) the real and imaginary parts of $1 - exp(-z\sqrt{i\nu/\omega}$ are plotted. For $z > 5\sqrt{\nu/\omega}$ the effects of the boundary become insignificant and the flow is essentially irrotational. For this reason the Stokes layer thickness is taken to be, by convention,

$$\text{Sttokes layer} \sim 5\sqrt{\nu/\omega}\ . \tag{32}$$

The z component of the velocity within the Stokes layer, required by the equation of continuity or incompressibility, is then

$$v = inU\left(-z + (1 - e^{-z\sqrt{i\omega/\nu}})\sqrt{\frac{\nu}{i\omega}}\right)\ . \tag{33}$$

[7]It is understood that velocities in this section are the real part of the given complex quantity.

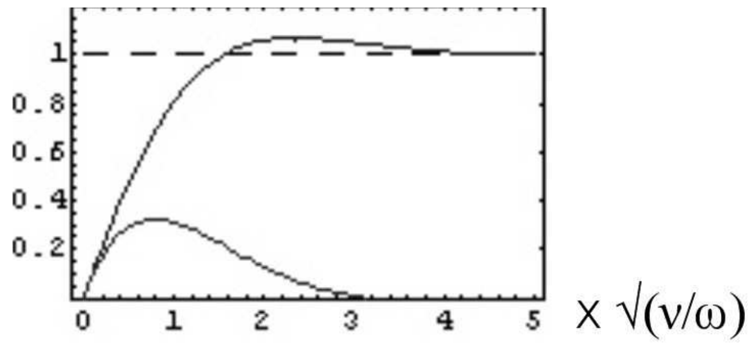

FIGURE 7. Estimate of the Stokes layer.

The force due to Reynolds stress (28) in the direction of x is

$$F_x = -\partial(\rho\overline{u}^2)/\partial x - \partial(\rho\overline{uv})/\partial z. \tag{34}$$

The first term on the right side of this equation represents the rate of increase of x-momentum (per unit volume). In the present case of a traveling wave $\overline{u}^2$ is independent of x and this term contributes no forcing.

Steady streaming with velocity u_L at the edge of the boundary layer in the x-direction results from $F_x - F_x^{inv}$ where F_x^{inv} is the inviscid part of F_x that leads to no net streaming. Within the Stokes boundary layer the only significant force opposing $F_x - F_x^{inv}$ is due to viscous stress. The steepest gradient of the viscous stress is in the z-direction so $\mu\Delta\overline{u}$ is dominated by the term $\mu\partial^2(\overline{u})\partial z^2$ and the mean streaming velocity at the edge of the boundary layer satisfies

$$F_x - F_x^{inv} + \mu\partial^2(\overline{u})\partial z^2 = 0, \tag{35}$$

which can be integrated to obtain the streaming velocity just outside the boundary layer,

$$u_L = -\frac{5}{4}n\omega U^2. \tag{36}$$

We remark that for a standing wave in a fluid, given by the real part of $u = U(x)e^{i\omega t}$, one gets the classical Rayleigh's law of streaming (see [27])

$$U_L = -3/(4\omega)U(x)U'(x). \tag{37}$$

In this case both terms of (34) are nonzero with the first contributing $-(4\omega)^{-1}U(x)U'(x)$ and the second contributing $-(2\omega)^{-1}U(x)U'(x)$.

REFERENCES

[1] A. Ahuja, J.A. Taylor, V. Lifton, A.A. Sidorenko, T.R. Salamon, E.J. Lobaton, P. Kolodner, T.N. Krupenkin, *Nanonails: A Simple Geometrical Approach to Electrically Tunable Superlyophobic Surfaces,* Langmuir **24** (2008,) 9–14.

[2] H. Antil, A. Gantner, R.H.W. Hoppe, D. Koster, K. Siebert, A.Wixforth, *Modeling and Simulation of Piezoelectrically Agitated Acoustic Streaming on Microfluidic Biochips*, in U.Langer, M. Iscacciati, D.E. Keyes, O. B. Widlund, W. Zulehner, eds., Domain Decomposition Methods in Science and Engineering XVII, Springer, 2008.

[3] J. Ashmore, *Cochlear Outer Hair Cell Motility*, Physiol. Rev. 88 (2008) 173-210.

[4] A. Bell and N.H. Fletcher, *The cochlear amplifier as a standing wave: "squirting" waves between rows of outer hair cells?*, J. Acoust. Soc. Am. **116** (2004), 1016-1024.

[5] J. R. Blake, *A spherical envelope approach to ciliary propulsion*, J. Fluid Mech. **46(1)** (1971), 199-208.

[6] B. Brahamsha, *Non-flagellar swimming in marine Synechococcus*, J. Molec. Microbiol. Biotechnol. **1** (1999), 59–62.

[7] F. Caicci, P. Burighel, L. Manni, *Hair cells in an ascidian (Tunicata) and their evolution in chordates*, Hearing Research **231(1-2)** (2007), 63–72.

[8] S. Childress, *Mechanics of Swimming and Flying*, Cambridge University Press, 1978.

[9] Y.T. Didenko, K.S. Suslick, *The energy efficiency of formation of photons, radicals and ions during single-bubble cavitation*, Nature **418** (2002), 394–397.

[10] R.W. Drum, R. Gordon, Star Trek replicators and diatom nanotechnology, Trends in Biotechnology **21(8)** (2003), 325–328.

[11] K.M. Ehlers, A.D.T. Samuel, H.C. Berg, R. Montgomery, *Do cyanobacteria swim using traveling surface waves?*, Proc. Natl. Acad. Sci. USA, **93** (1996), 8340–8343.

[12] Fair, MC, Anderson, JL, *Electrophoresis of Nonuniformly Charged Ellipsoidal Particles*, Journal of Colloid and Interface Science, **127(2)** (1989).

[13] R. Feynman, *There's plenty of room at the bottom*, Eng. and Science **23(5)** (1960), 22–36. $http://www.its.caltech.edu/\ feynman/plenty.html$.

[14] T. Frommelt, M. Kostur, M. Wenzel-Schfer, P.Talkner, P. Hanggi, A. Wixforth, *Microfluidic mixing via acoustically driven chaotic advection*, Phys. Rev. Lett. **100(3)** (2008), 034502.

[15] A. Gantner, R.H.W. Hoppe, D. Koster, K. Siebert, A.Wixforth, *Numerical simulation of piezoelectrically agitated surface acoustic waves on microfluidic biochips*, Comput. Visual Sci., **10** (2007), 145–161.

[16] R.Gordon, F. Sterrenburg, K. Sandhage, *Special Issue on Diatom Nanotechnology*, J. Nanoscience and Nanotechnology **5(1)** (2005), 1–178.

[17] J. Guasto, K. Breuer, *Micro-velocimetry using time-resolved measurements of quantum dots in a microchannel.* ECI International Conference on Heat Ttransfer and Fluid Flow in Microscale, Whistler, 2008.

[18] K.F. Jarrell, M.J. McBride, *The surprisingly diverse ways that prokaryotes move*, Nature Reviews: Microbiology **6(6)** (2008), 466–476.

[19] F. Jülicher, *Mechanical Oscillations at the Cellular Scale*, C. R. Acad. Sci. (Paris) Ser. IV, **6** (2001), 849–860.

[20] K. D. Karavitaki, D. C. Mountain, Evidence for Outer Hair Cell Driven Oscillatory Fluid Flow in the Tunnel of Corti, Biophys. J., **92(9)** (2007), 3284–3293.

[21] J. Koiller, K. M.Ehlers, R. Montgomery *Problems and progress in microswimming*, J.Nonlinear Science, **6(6)** (1996), 1432–1467.

[22] J. Koiller, K.M. Ehlers, F. Chalub, *Acoustic streaming, the "small invention" of cyanobacteria?* Arbor (CSIC), to appear.

[23] D. Koster, *Numerical simulation of acoustic streaming on surface acoustic wave-driven biochips*, SIAM J. Sci. Comput., **29(6)** (2007), 2352–2380.

[24] D. Koster, *A boundary integral method for compressible Stokes flow*, Proc. Appl. Math. Mech., **8** (2008), 10975–10976.

[25] E. Lauga, T.R. Powers, *The hydrodynamics of swimming microorganisms*, arXiv:0812.2887, submitted.
[26] J. Lighthill J, *On the squirming motion of nearly spherical deformable bodies through liquids at very small Reynolds numbers*, Comm. Pure and Appl. Math., **5** (1952), 109–118.
[27] J. Lighthill, *Acoustic streaming*, J. Sound Vib., **61(3)** (1978), 391–418.
[28] J. Lighthill, *Waves in fluids*, Cambridge University Press, 1978 (second edition 2001)
[29] J. Lighthill, *Acoustic streaming in the ear itself*, J. Fluid Mechanics, **239** (1992), 551–606
[30] J. Lighthill, *Biofluiddynamics: A Survey*, in A.Y. Cheer, C.P. van Dam, editors, Fluid Dynamics in Biology, American Mathematical Society, 1993.
[31] G. Lindner, *Sensors and actuators based on surface acoustic waves propagating along solidliquid interfaces*, J. Phys. D: Appl. Phys., **41** (2008), 123002.
[32] M.S. Longuet-Higgins, *Mass transport in water waves*, Phil Trans. R. Soc. London Ser. A, **245** (1953), 535–581.
[33] B.R. Lutz, J. Chen, D.T. Schwartz, *Microfluidics without microfabrication*, Proc. Natl. Acad. Sci., **100(8)** (2003), 4395--4398.
[34] V. Magar, T.J. Pedley, *Average nutrient uptake by a self-propelled unsteady squirmer*, J. Fluid Mechanics, **539** (2005), 93–112.
[35] P. Marmottant, S. Hilgenfeldt *A bubble-driven microfluidic transport element for bioengineering*, Proc. Nat. Acad. Sci., **101(26)** (2004), 9523–9527.
[36] P. Marmottant, J.P. Raven, J.G.E. Gardeniers, J.G. Bomer, S. Hilgenfeldt, *Microfluidics with ultrasound-driven bubbles*, J. Fluid Mechanics, **568** (2006), 109–118.
[37] J. McCarren, J. Heuser, R. Roth, N. Yamada, M. Martone, B. Brahamsha, *Inactivation of swmA Results in the Loss of an Outer Cell Layer in a Swimming Synechococcus Strain*, J. Bacteriol., **187(1)** (2005), 224230.
[38] J. McCarren, B. Brahamsha, *SwmB, a 1.12-megadalton protein that is required for non-flagellar swimming motility in Synechococcus*, J. Bacteriology, **189(3)** (2007), 1158–1162.
[39] R.M. Moroney, R.M. White, R.T. Howe, Appl. Phys. Lett., **59(7)** (1991), 774–776.
[40] W.L. Nyborg, *Acoustic Streaming near a Boundary*, J. Ac. Soc. America, **30(4)** (1958), 329–339.
[41] A. Pelling, S. Sehati, J. Gralla, J. Valentine, J. Gimzewski, *Local Nanomechanical Motion of the Cell Wall of Saccharomyces cerevisiae*, Science, **305** (2004), 1147–1150.
[42] T.P. Pitta, H. C. Berg, *Self-electrophoresis is not the mechanism for motility in swimming cyanobacteria*, J. Bacteriol., **177(19)** (1995), 5701–5703.
[43] T.P. Pitta, E.E. Sherwood, A.M. Kobel, H.C. Berg, *Calcium is required for swimming by the nonflagellated cyanobacterium Synechococcus strain WH8113*, J. Bacteriol., **179(8)** (1997), 2524–2528.
[44] G. Popescu, Y.K. Park, W. Choi, R.R. Dasaria, M.S. Feld, K. Badizadegan, *Imaging red blood cell dynamics by quantitative phase microscopy*, Blood Cells, Molecules, and Diseases, **41(1)** (2008), 10–16.
[45] E.M. Purcell, *Life at Low Reynolds Number*, American Journal of Physics, **45** (1977), 3–11.
[46] Lord Rayleigh, *The Theory of Sound*, 1877 (1945 edition, Dover, New York).
[47] Lord Rayleigh, *On the circulation of air observed in Kundts tubes, and on some allied acoustical problems*, Phil. Trans., **175** (1883), 1–21.
[48] Lord Rayleigh, *On Waves Propagated along the Plane Surface of an Elastic Solid*, Proc. London Math. Soc.,**1-17** (1885), 4–11.
[49] A. Renaudin, P. Tabourier, V. Zhang, J.C. Camart, C. Druon, *SAW nanopump for handling droplets in view of biological applications*, Sensors and Actuators B 113 (2006) 389–397.
[50] N. Riley, *Steady Streaming*, Annual Review of Fluid Mechanics, **33** (2001), 43–65.

[51] A.D.T. Samuel, J. Petersen, T. Reese, *Envelope structure of Synechococcus sp. WH8113, a nonflagellated swimming cyanobacterium*, BMC Microbiology 1(4) (2001)
[52] A. Shapere, F. Wilczek, *Geometry of self-propulsion at low Reynolds number*, J. Fluid Mechanics, **198** (1989), 557–585.
[53] J. Sznitman, T. Roesgen, *Acoustic streaming flows in a cavity: an illustration of small-scale inviscid flow*, Physica D **237** (2008), 2240–2246.
[54] T.M. Squires, S.R. Quake, *Microfluidics: Fluid physics at the nanoliter scale*, Rev. Mod. Phys. **77** (2005), 977–1026.
[55] H.A. Stone, A.D.T. Samuel, *Propulsion of micro-organisms by surface distortions*, Phys. Rev. Let. **77** (1996), 4102–4104.
[56] C. Suria, K. Takenaka, H. Yanagida, Y. Kojima, K. Koyama, *Chaotic mixing generated by acoustic streaming*, Ultrasonics **40** (2002), 393–396.
[57] J.B. Waterbury, J.M. Willey, D.G. Franks, F.W. Valois, S.W. Watson, *A cyanobacterium capable of swimming motility*, Science **230** (1985), 74–76.
[58] R.L. Weaver, O.I. Lobkis, A. Yamilov, *Entrainment and stimulated emission of ultrasonic piezoelectric auto-oscillators*, J. Acoust. Soc. Am. **122(6)** (2007), 3409–3418.
[59] A. Wixforth, C. Strobl, C. Gauer, A. Toegl, J. Scriba , Z. v. Guttenberg, *Acoustic manipulation of small droplets*, Anal. Bioanal. Chem. **379** (2004), 982--991.
[60] J. Wu, W. Nyborg, *Ultrasound, cavitation bubbles and their interaction with cells*, Advanced drug delivery reviews **60(10)** (2008), 1103–1116.

Kurt M. Ehlers
Truckee Meadows Community College
7000 Dandini Blvd, Reno
NV 89512, USA
E-mail address: `kehlers@tmcc.edu`

Jair Koiller
Centro de Matemática Aplicada
Fundação Getulio Vargas
Rio de Janeiro, RJ 22250-020, Brazil
E-mail address: `jair.koiller@fgv.br`